# Flow rate distribution and effect of convection and radiation heat transfer on the temperature profile during a coil annealing process

Abdallah Haouam, Maxence Bigerelle

# Flow rate distribution and effect of convection and radiation heat transfer on the temperature profile during a coil annealing process

**A. Haouam · M. Bigerelle**

**Abstract** Determining the temperature of several steel coils, heated in a furnace with a controlled hydrogen environment is important in an annealing process. Temperatures must be defined during heat treatment in order to guarantee metallurgical properties and acceptable reduced residual stresses. In this paper we approach hydrogen flow characteristics in the furnace and through a set of coils using an annealing non-differential model. Fluid flow is schematized as a pipe network solved by the Hardy Cross method to obtain pressure drops across the various gas flow segments. A comparison is made between measured and simulated results, confirming the adequacy of adopted assumptions and the validity of proposed model. Convective and radiative exchanges between the furnace and the coils are calculated by a discretization using the finite differences method. The convection coefficients are estimated and introduced into the boundary conditions around the coil to obtain the temperature distribution in the coils and in the covering bell. Finally, heat exchanges by convection and radiation are estimated by this model and the modeling errors are <8 °C.

**List of symbols**

| | |
|---|---|
| $Nb$ | Number of coils |
| $N_c$ | Number of discretization points |
| $Nu$ | Nusselt number |
| $Re$ | Reynolds number |
| $Pr$ | Prandtl number |
| $L$ | Length (m) |
| $D_H$ | Hydraulic diameter (m) |
| $A$ | Section of the pipe ($m^2$) |
| Q | Flow rate in the pipe ($m^3/s$) |
| $U$ | Gas velocity (m/s) |
| $Cv_i$ | Number of channels in the $i$th convector |
| $q_i$ | Flow rate in a stylized branch $i$ |
| $P_i$ | Pressure drop in the branch $i$ (Pa) |
| $r_i$ | Coil interior radius (m) |
| $r_e$ | Coil exterior radius (m) |
| $r_b$ | Bell interior radius (m) |
| $r_{cg}$ | Gas cane radius (m) |
| $x_{cg}$ | Gas cane height (m) |
| $b_i$ | Burner coefficient |
| $t$ | Time (s) |
| $T$ | Temperature (K) |
| $T_{cg}$ | Temperature of the gas cane |
| $T_b$ | Temperature of the bell vis-a-vis the gas cane |
| $T_b$ | Temperature of the coil vis-a-vis the gas cane |
| $S$ | Surface ($m^2$) |
| $F_{S1-S2}$ | Factor form of surface $S_1$ towards surface $S_2$ |
| $F_{c-cg}$ | Factor form of the coil towards the gas cane |
| $F_{b-cg}$ | Factor form of the bell towards the gas cane |
| $k$ | Thermal conductivity (W/m °C) |
| $h$ | Convection coefficient ($W/m^2$ °C) |
| $h_{cg}$ | Convection coefficient of the gas cane |
| $h_b$ | Convection coefficient of the bell |
| $h_c$ | Convection coefficient at the external radius coil |
| $h_{hp}$ | Convection coefficient of high pile |
| $h_{lp}$ | Convection coefficient of low pile |
| $h_{ey}$ | Convection coefficient at coil core (eye coil) |
| $h_{sp}$ | Convection coefficient at the coil section |

A. Haouam (✉)
Mechanical Engineering Department, Badji Mokhtar University,
PO Box 12, 23000 Annaba, Algeria
e-mail: haouam_a@yahoo.fr

M. Bigerelle
Laboratory of Research TEMPO, EA 4542, University
of Valenciennes and Hainaut-Cambresis,
59300 Valenciennes, France
e-mail: maxence.bigerelle@univ-valenciennes.fr

**Greek symbols**

| | |
|---|---|
| $\Delta r$ | Step discretization (*axis r*) (m) |
| $\Delta z$ | Step discretization (*axis z*) (m) |
| $\Delta x$ | Differential element |
| $\lambda$ | Regular pressure drop coefficient |
| $\chi_i$ | ith Singular pressure drop coefficient |
| $\rho$ | Density (kg/m$^3$) |
| $\mu$ | Dynamic viscosity (Pa s) |
| $\varepsilon_{cg}$ | Cane gas emissivity |
| $\varepsilon_g$ | Gas emissivity |
| $\varepsilon_b$ | Bell emissivity |
| $\varphi$ | Radiative flux (W/m$^2$) |
| $\sigma$ | Stephan–Boltzman constant, $5.67 \times 10^{-8}$ (W/m$^2$ K$^4$) |
| $\theta_0^b$ | Bell wall temperature at the level of the gas cane (°C) |
| $\theta_0^{b^n}$ | Bell wall temperature at the *n*th iteration (°C) |
| $\theta_x^b$ | Bell temperature at a height *x* of the gas cane (°C) |
| $\theta_g$ | Gas cane temperature (°C) |
| $\xi_g$ | Maximum variation tolerated for $\theta_0^{cl}$ |
| $\zeta_{fl}$ | Maximum deviation tolerated speeds (%) between two iterations of Newton–Raphson |

**Indices**

| | |
|---|---|
| b | Bell |
| c | Coil |
| g | Gas |
| cg | Cane gas |
| hp | High pile |
| lp | Low pile |
| ey | Eye of coil |
| sp | Spacer |

## 1 Introduction

Annealing of steel coils is done to alter the crystal structure of the steel which can become brittle during cold rolling. During this process the whole coil must be heated to the required temperature and then maintained at this temperature for a period of time. For these reasons, modeling of gas flow and associated heat fluxes in heat treatment furnaces is of great importance for prediction and control of work piece ultimate microstructure. The heat transfer phenomena in annealing furnaces of high performance using hydrogen were studied by several authors, in particular Jaluria [1], Sabbonchi et al. [2] and Zou et al. [3]. For these authors, the numerical simulation of the heat transfer and fluid processes in a furnace was carried out using a finite-difference method. They determined the best arrangement of coils loaded with the shortest heating time. In the same way, Tagliafico et al. [4] have also used a numerical model based on a finite difference technique to simulate thermal behavior of coils. Sahay and Kumar [5] developed a model capable to predict variations in temperature, microstructure and mechanical properties of different coils annealed in batch annealing furnaces. The heating process in a database of simulated annealing was also carried out by Azimian et al. [6] involving the effects of various parameters such as inlet temperature, type of used gas, fan power, coil size and weight. This allowed obtaining the temporal variation of critical temperature points defined as the temperature at the hot and cold spots of the annealing base. In order to know the incidence of annealing on the quality of the products and the total productivity of the cold rolling mill, Tata Steel produced a data-processing simulator having the capacity to predict the temporal and space evolution of the temperature, the microstructure and the mechanical properties of the various steel coils [7].

The objective of this study is to model the gas flow in the annealing base using a simple approach on Bernoulli equations and Hardy cross method [8], and to determine the gas temperature distribution within the gas circuit itself by modeling the convective and radiative heat fluxes.

## 2 Physical description

In many batch annealing furnace designs, annealing is carried out for several coils stacked one above the other forming a single pile as shown in Fig. 1. The format of coils in a base is variable and depends on the desired future use. The height usually varies from 500 to 1,400 mm, inner diameter from 500 to 600 mm, outer diameter from 1,200 to 2,200 mm and thickness from 0.3 to 3 mm. Therefore the number of coils in the database varies from 3 to 6 and the coils are separated by convectors. The stack is capped by a bell in which circulates a protection gas (hydrogen or nitrogen) to avoid any phenomenon of oxidation during annealing operations. A furnace consisting of 6 burners facing the first coil fits over the entire load and ensures gradual heating. The burners use natural gas and are set to deliver a fixed amount of heat (600 kW) when furnace nozzles are at their maximum apertures. To avoid problems of oxidation, the basis of annealing is swept by a reducing gas with respect to oxygen (4–5 m$^3$/s). For security reasons, the plant uses 2 protective gases: nitrogen (with 5 % hydrogen) and pure hydrogen. The advantage of using hydrogen rather than nitrogen is summarized in three points: (1) better thermal conductivity of hydrogen compared to that of nitrogen (ten times higher), (2) hydrogen is lighter than nitrogen, the fan will consume less energy and (3) ultimately hydrogen combines with the residual carbon present on the surface of the steel to form methane, thus cleaning the exposed surface. The circulation of protective gas is assured by a centrifugal fan. In order to control the

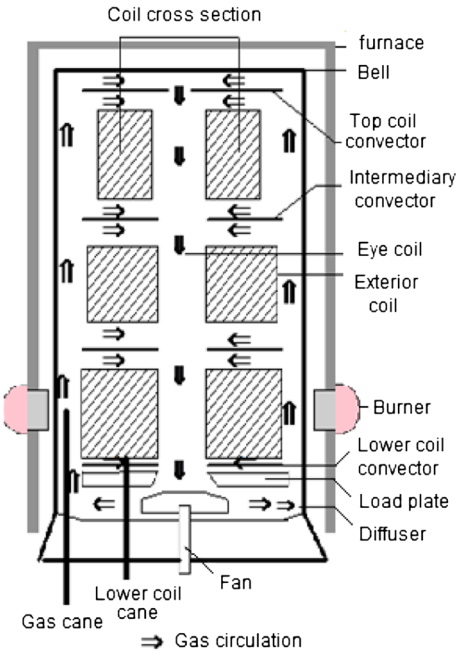


**Fig. 1** Batch annealing furnace design

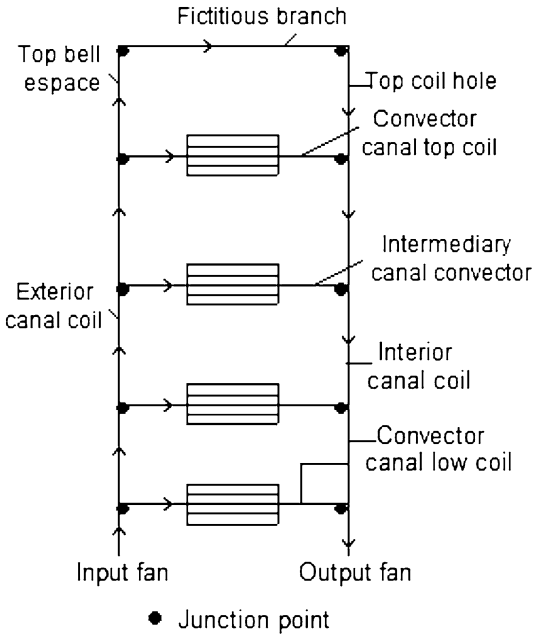


**Fig. 2** Flow distribution in the annealing furnace

temperature of the gas, rod gas thermocouples are placed in front of the burners between the first coil and the protective cover. Temperature measurements are introduced into a control loop PID which activates the simultaneous opening or closing of the burners based on a predetermined reference temperature.

## 3 Gas flow modeling

In most parts of the circuit followed by the gas, the hydrodynamic regime is turbulent. Thus, integration of the Navier–Stokes equations becomes prohibitive in computing time. Instead of reasoning on integral equations, quite general, we will use Bernoulli equations, applicable in particular cases.

### 3.1 Schematization

The convector is composed of several branches allowing gas passage as illustrated in Fig. 2. Different parts of the gas circuit inside the furnace are schematized as a system of pipes with particular cross-sections in order to use a solving tool such as Hardy Cross method. Suppose that the gas circuit in the base can be considered as a network of $n$ loops, $p$ branches, containing $p$ unknown flow rates (Fig. 3). From the flow conservation equations, we obtain a system of $k$ nonlinear equations with $k$ unknowns, where $k$ depends on the number of bifurcations in the system

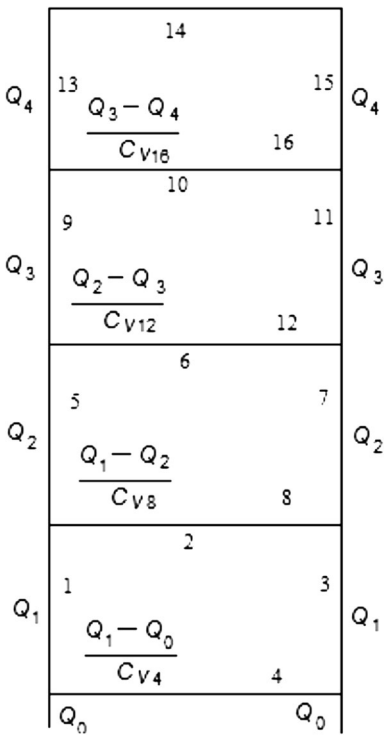


**Fig. 3** Flow model within inner cover

concerned. This system is not a linear system because the pressure drops are not linear functions of the flow. We use a numerical method for solving nonlinear systems based on the following restrictions:

- Incompressible flow.
- Rotational symmetry of the fluid movement (the coils, the convectors and the protective bell are centered on the axis of the fan which becomes the axis of revolution of this system).
- Knowledge of fan flow, knowledge of pressure drop and the average speed obtained (no velocity distribution in the section of the pipe).
- For each branch of the circuit, depending on the velocity and the relative roughness of the pipe wall (assessed by feel rugosimetry), the regular and singular pressure drops are estimated.

### 3.2 Pressure drop calculation along a circuit branch

For each branch of the circuit, depending on the velocity and the relative roughness ε of the pipe wall, the pressure drops have the general expression [9]:

$$J = \left\{ \frac{\lambda L}{D_h} + \sum_{i=1}^{n} \chi_i \right\} \frac{\rho Q^2}{2A^2} \tag{1}$$

where λ is determined by Reynolds Number, which imposes the choice of thermal convection expressions. Using mementos and books [9–12], expressions for the pressure drop coefficients $\chi_i$ at all the singularities encountered in the base of annealing are obtained (Appendix 1).

### 3.3 Calculation of flow rates in the base

The number of coils varies from one annealing operation to another. Consequently, the geometry of a stack of coils differs substantially at each annealing. For the case of annealing with 3 coils (Fig. 3), the circuit branches are numerated from 1 to 16. In fact, branch 2 is identical to branch 8 and likewise, branch 6 is identical to branch 12. In this case, the 14th branch seeing no pressure drop is assumed to have zero flow. Furthermore, branch 14 can simplify the formulation and the numerical calculation of flows in the base. The number of branches in the ith coil, the flow in the branch, the flow described in the diagram, isolating the mesh and by conservation of flow:

$$Q_0 = Q_1 + C_v q_4 \tag{2}$$

This leads for the branches 1–4 to the following equations:

$$q_1 = Q_1 \tag{3}$$

$$q_3 = Q_1 \tag{4}$$

$$q_2 = \frac{Q_2 - Q_1}{C_{V2}} \tag{5}$$

The relations are extended to *Nb* coils (*Nb* + 1 *mesh points*) giving then (*Nb* + 1) unknown flows $Q_1, Q_2, \ldots Q_{Nb+1}$. Let the pressure drop in the branch, defined by the Colebrook curves [9] for a flow and singular pressure drops in the industry, the pressure equilibrium in the mesh 1 leads to the relationship:

$$P_1 + P_2 + P_3 - P_4 = 0 \tag{6}$$

and we get the generalized pressure drop equations:

$$\sum_{i=1}^{3} \left( P_{4(j-1)+i} - P_{4j} \right) = 0, \quad j \in 1, 2 \ldots Nb + 1 \tag{7}$$

To solve this system of nonlinear equations, an iterative method based on Newton's method is used. The Jacobian is calculated numerically by an increment $\Delta = 10^{-6}$ and a standard stop is fixed at $\xi_{fl}$ as:

$$\left\| \frac{Q^{n+1} - Q^n}{Q^n} \right\| < \xi_{fl}. \tag{8}$$

## 4 Flow modeling results

### 4.1 Flow measurements

The centrifugal fan delivers 55,000 $m^3$/h under vacuum at 1,477 Pa for 1,450 rev./min. Experimental measurements show that the gas has no significant temperature gradient within the base and thus its density is constant while leaving invariant the operating point. The fan is thermally neutral as it does not cool the gas. LOI society, reproducing a model in 1/3, developed a pressure flow curve for a conventional charge in hydrogen at 20 °C [13] (Fig. 4). Several loads are created by variation of the coils number, their radius and their heights. By fixing several fan speeds and two temperatures (0 and 700 °C), the total pressure drop in the base is obtained by summation of all pressure drops (Table 1). Plotting the characteristic curves of the pressure drops in the base at temperature of 0 °C; under the conditions that were used to establish the fan pressure drop-flow curve (Fig. 5). It appears that the LOI

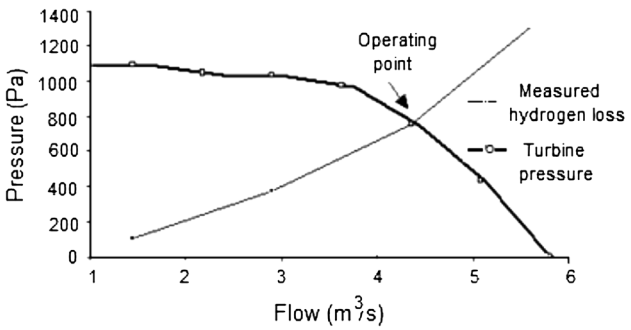


**Fig. 4** Pressure-flow curve for a conventional charge in hydrogen at 20 °C

**Table 1** Pressure drop in the annealing base

| $T_g$ (°C) | | 20 | 20 | 20 | 20 | 700 | 700 | 700 | 700 |
|---|---|---|---|---|---|---|---|---|---|
| Number of coils | | 3 | 4 | 5 | 6 | 3 | 4 | 5 | 6 |
| Fan flow ($m^3/s$) | Pressure drop (Pa) | | | | | | | | |
| 1.527 | 78 | 71 | 67 | 65 | 57 | 60 | 62 | 63 | |
| 3.054 | 292 | 243 | 218 | 206 | 156 | 156 | 156 | 158 | |
| 4.581 | 696 | 565 | 489 | 446 | 287 | 279 | 276 | 276 | |
| 6.108 | 1,300 | 1,057 | 915 | 822 | 448 | 428 | 419 | 415 | |
| 7.635 | 2,101 | 1,740 | 1,503 | 1,344 | 640 | 602 | 584 | 575 | |
| 9.162 | 3,082 | 2,584 | 2,245 | 2,014 | 865 | 802 | 771 | 755 | |

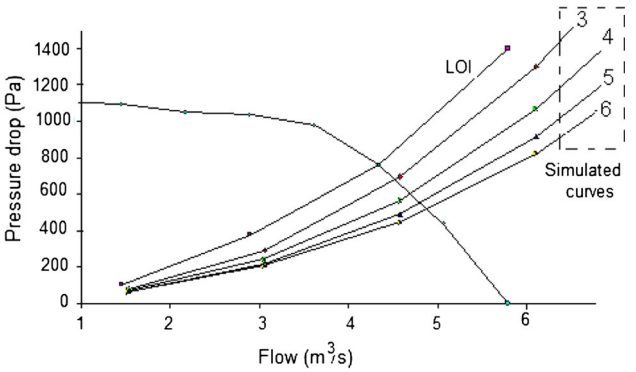


**Fig. 5** Pressure drop in the batch annealing furnace under hydrogen flow at 20 °C for different number of coils

experimental curve has a growth rate slightly higher than the simulated curves. The area of operation varies between 4.5 and 4.9 $m^3/s$, depending of the number of the coils in the base. For a large number of coils there is an increase in the number of convectors and thus a reduction in flow causing a decrease in pressure drops. The flow for each operating point is calculated by binary search. A nonlinear regression of flows depending on the number of coils gives (Fig. 6):

$$q_0 = 3.996(Nb)^{0.1144} \tag{9}$$

Grundman measured the flow of hydrogen over a database LOI containing 6 coils [13]. The gas temperature is 25 °C and flow fan 15,300 $m^3/h$ (16,500 $m^3/h$ for the model). Flows are measured on the upper half and lower of the convector. The tests were conducted in two geometrical configurations as follows:

- There is no flow in the center of the top coil (Fig. 7): we note that our model fits well with the reality without any calibration and therefore the losses estimated in the convector, in the eye of the coils and between the bell and the coils are correct.

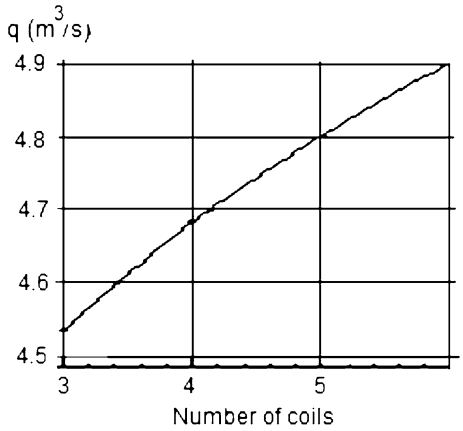


**Fig. 6** Fan flow curve versus the number of coils

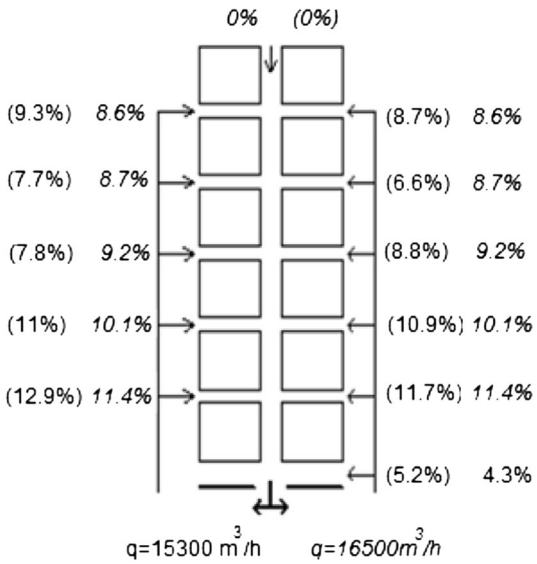


**Fig. 7** Measured and calculated (*italic*) flows with no flow in the center of the top coil

- The flows are determinate without top coil convector (Fig. 8): to simulate the absence of top coil convector we increase the pressure drop of fluid flowing through it excessively. We note also a good fit of the model with experimental results. Modeling is reliable and gives errors of <2 % compared to measurements.

## 4.2 Assessment of pressure drops

Kawasaki Steel designed a model of a base to 1/3 and measured the pressure drop across the convectors by varying their height [14]. These tests were performed at room temperature under a nitrogen atmosphere. The pressure curves in the convectors under different flow rates are given. The pressure drop in the convectors is measured for

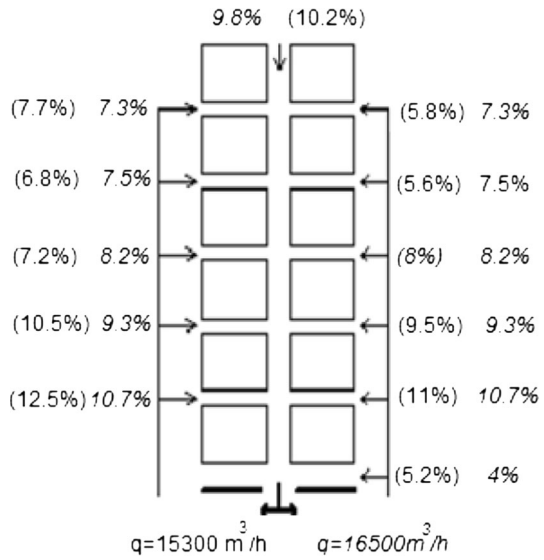


**Fig. 8** Measured and calculated (*italic*) flows without top coil convector

different heights: 8.3; 11.7; 23.3; 31.7; 46.7 and 60 mm$H_2O$ (Fig. 9a). By taking the thermo physical parameters of nitrogen, the fan speed is varied for each flow in the convector where the height is imposed (the shape of the convector is unknown). Then it is possible to obtain the evolution of the flow based on pressure drops for a given height (Fig. 9b). There is a rather marked similarity between the flow modeling and Kawasaki Steel testing. The slopes of experimental and modeled curves are identical; the relationship pressure drop-flow is validated.

## 5 Gas temperature modeling

The iterative method used is close to that of the resolution using differential connections [15–17]. By supposing known the approximate result of a model at the moment $t$, one can calculate the other temperatures at the moment $t$. Using the values of these models, one can recomputed the first model, always taken at the moment $t$. One then renews this iterative process until convergence of the models towards an eigenvalue $\xi$ considered to be acceptable. One can thus recompute the model at the moment $(t + \Delta t)$ and renew the preceding iterative process. The models will, as follows, calculate the temperatures in certain points of the annealing base (Fig. 1). Heat exchanges occurring within the base of annealing are:

- *Convective exchanges* The colder gas in the ventilator is heated by licking the bell and yields calories to the coils as with the other parts of the base (convector, load plate…).

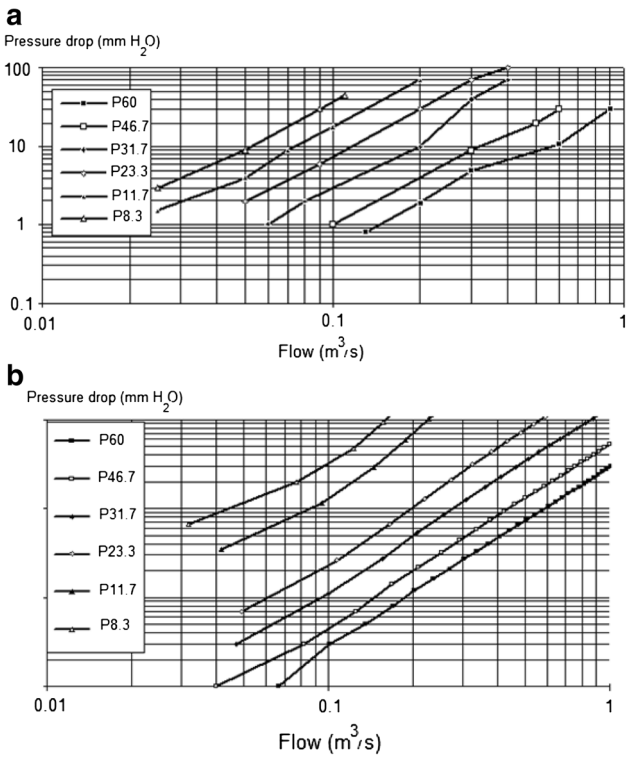


**Fig. 9** **a** Relation between air flow rate and pressure drop measured in the convector for different heights of convector rib. **b** Relation between air flow rate and pressure drop modeled in the convector for different heights of convector rib

- *Radiative exchanges* Diatomic gases with symmetrical molecules, such that of nitrogen and hydrogen do not radiate in the fork of temperature of annealing. So, the protection gas of annealing does not intervene in the radiative exchanges.

### 5.1 Convective fluxes modeling

#### *5.1.1 Heat transfer equations*

The following simplifying assumptions are made:

- The gas does not absorb radiated heat.
- For a perpendicular section, velocity of gas and its temperature will be constant.
- Physical and thermal parameters depend on the temperature and the gas nature.
- The ventilator does not modify the gas temperature.

Thus, heat exchange can be schematized by a fluid circulating between 2 walls. By considering a control volume of gas, the expression of the differential of the energy absorbed by gas $\delta Q$, of flow $q$ of heat-storage capacity $c$, on a course $[x, x + \delta x]$ during a time $\delta t$, licking the 2 walls ($p1$, $p2$) of surface $(\delta S_1, \delta S_2)$ is written:

$$\delta Q = \left[h_{1,x}\left(\theta_{p1,x} - \theta_x\right)\delta S_1 + h_{2,x}\left(\theta_{p2,x} - \theta_x\right)\delta S_2\right]\delta t \quad (10)$$

where $h_1$ and $h_2$ are convection coefficients.

The rise in temperature of the volume $\delta V$ is due to the energy yielded or provided by the 2 faces, hence

$$\delta Q = \rho c q \frac{\partial \theta_x}{\partial x}\delta x \delta t \quad (11)$$

$$\frac{\partial \theta_x}{\partial x} = \frac{1}{\rho_x c_x q_x}\left[h_{1,x}\left(\theta_{p1,x} - \theta_x\right)l_1 + h_{2,x}\left(\theta_{p2,x} - \theta_x\right)l_2\right]. \quad (12)$$

This differential equation cannot be solved analytically owing to the fact that $\theta_p$ depends on $x$ (the temperatures of bell and coils surfaces and the flows are not uniform along the gas path), $h$ depends on $\theta_x$ and on $x$, just as $c$ and $\rho$ depend on the gas temperature. Discretized by the finite difference method, this equation is written as:

$$\theta_{x+\Delta x} = \theta_x + \frac{\Delta x}{\rho_x c_x q_x} \times \left[h_{1,x}\left(\theta_{p1,x} - \theta_x\right)l_1 + h_{2,x}\left(\theta_{p2,x} - \theta_x\right)l_2\right] \quad (13)$$

*Bell-external coil equation (position Nb)*

$$\theta_{z+\Delta z} = \theta_z + \frac{2\pi \Delta z}{\rho_z c_z q_z} \times \left[h_{b,z}\left(\theta_{b,z} - \theta_z\right)r_b + h_{c,z}^{Nb}\left(\theta_{c,z}^{Nb} - \theta_z\right)r_e^{Nb}\right] \quad (14)$$

The resolution of equation requires the knowledge of the temperature in a point which will be that of the regulation cane. The convection coefficient $h$ is obtained by the correlation characterizing the turbulent flows of gases in channels of annular section [18]:

$$Nu_f = 0.017 Re_f^{0.8} Pr_f^{0.4}\left[\frac{Pr_f}{Pr_p}\right]^{0.25}\left[\frac{r_b}{r_e}\right]^{0.8} \quad (15)$$

with

$$Nu = \frac{hL}{k} \quad (16)$$

where $L$ is a characteristic length equal to the equivalent diameter $2(r_b - r_e)$ and $k$ the thermal conductivity.

*Convector equation between coils Nb and Nb − 1*

$$\theta_{r+\Delta r} = \theta_r + \frac{\Delta r}{\rho_r c_r q_r} \times \left[h_{cv,r}^{Nb}\left(\theta_{c,r}^{Nb} - \theta_r\right)S_r + h_{cv,r}^{Nb}\left(\theta_{c,r}^{Nb-1} - \theta_r\right)S_r\right] \quad (17)$$

In the case of the convector, $S_r$ is not constant and it evolves according to $r$. To obtain $h_{cv}$, one will use the Dittus Boelter correlation characterizing turbulent flows of a gas in a tube [13]:

$$Nu_f = 0.023 Re_f^{0.8} Pr_f^{0.4} \quad (18)$$

*Top coil convector equation*

The top coil convector exchanges heat only with the last coil. So the formula becomes:

$$\theta_{r+\Delta r} = \theta_r + \frac{\Delta r}{\rho_r c_r q_r}\left[h_{hp,r}\left(\theta_{c,r} - \theta_r\right)S_{hp,r}\right] \quad (19)$$

Because of the similar configuration of the highest convector of pile, the correlation of Kays is used (turbulent flows of gases in rectangular tubes) [14]:

$$Nu_f = 0.023 Re_f^{0.8} Pr_f^{0.33} \quad (20)$$

*Low coil convector equation*

The low coil convector exchanges heat only with the first coil. So the formula is:

$$\theta_{r+\Delta r} = \theta_r + \frac{\Delta r}{\rho_r c_r q_r}\left[h_{lp,r}\left(\theta_{c,r} - \theta_r\right)S_{bp,r}\right] \quad (21)$$

$$Nu_f = 0.023 Re_f^{1.8} Pr_f^{2.5} \quad (22)$$

*Coil central region equation*

$$\theta_{z+\Delta z} = \theta_z + \frac{2\pi r_i \Delta z}{\rho_r c_r q_r}\left[h_{ey,z}\left(\theta_{c,z} - \theta_z\right)\right] \quad (23)$$

$$Nu_f = 0.023 Re_f^{0.8} Pr_f^{0.4} \quad (24)$$

The gas flowing in top of the eye of a coil is the mixing of a gas flow $Q_1$ resulting from the eye of the top of the coil and of a gas flow $Q_2$ from the convector. The required initial temperature to calculate the gas temperature in the eye of the coil is the temperature resulting from these two flows. The instantaneous mixture of gases will give a gas flow having an average temperature:

$$\theta_{nz(ey)}^{Nb-1} = \frac{\theta_{0(ey)}^{Nb} Q_2 + \theta_{0(sp)}^{Nb} Q_1}{Q_1 + Q_2}. \quad (25)$$

### 5.2 Determination of the bell temperature

One will choose a "thermo-statistical" approach in order to determine the temperature of the bell. This method consists in determining the profile of the bell temperature using a reference point (the gas cane temperature), located at the hottest place of the base. A test was carried out to position 3 thermocouples outside the bell (Fig. 10). Assuming that the bell temperature is related to its height and is a function of the heat flux in the form:

$$\theta_x^b = \theta_0^b + f(\varphi, x) \quad (26)$$

where φ represents the heat flux yielded by the bell vis-a-vis of the gas cane in $\theta_0^b$. $\theta_x^b$ is the temperature of the bell at a height $x$ from the position of the gas cane; $f$ is a function to be determined. The net heat flux leaving the bell at the point where $\theta_0^b$ is known to heat the gas:

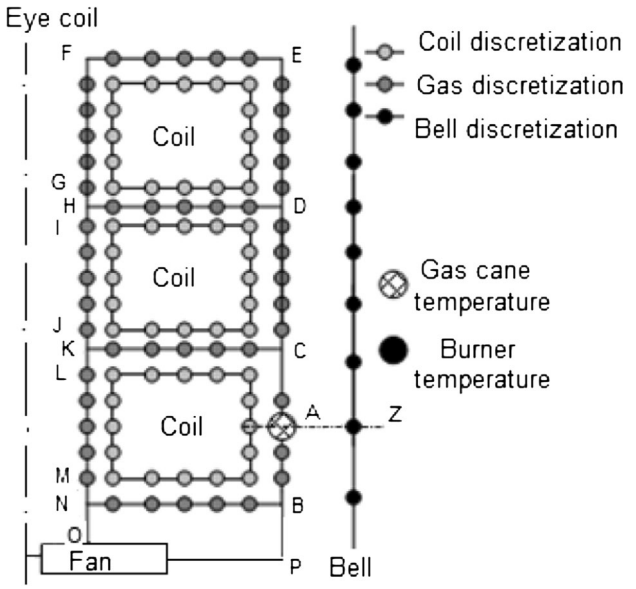


**Fig. 10** Sample points of the annealing furnace

$$\varphi = h_b\left(\theta_0^b - \theta_g\right) + b\varepsilon_g\varepsilon_b\left(T_0^{b^4} - T_g^{b^4}\right) \tag{27}$$

While neglecting the radiation between the bell and the coils, gas diathermic $\varepsilon_{gas} \approx 0$:

$$\varphi = h_b(\theta_b - \theta_g) \tag{28}$$

It would be necessary to find a function which satisfies $\theta_x^b$ maximum at $\theta_0^b$ and decreasing according to $|x|$, while imposing that $\theta_x^b$ to be a polynomial function of the flux density φ, which amounts to seeking an equation of the type:

$$\theta_x^b = \theta_0^b + \sum_{i=1}^{N} b_i\varphi^i|x| = \theta_0^b + \sum_{i=1}^{N} b_i\left(\theta_g - \theta_0^b\right)^i|x| \tag{29}$$

The characteristic coefficients $b_i$ for the burners is determined by a nonlinear regression using the experimental data and the good compromise between the number of coefficients of the model. The precision is obtained for $N = 2$

$$\theta_x^b = \theta_0^b + \left(\theta_g - \theta_0^b\right)|x| + b_2\left(\theta_g - \theta_0^b\right)^2|x|$$
$$b_1 = 9.79 \times 10^{-1} \pm 10^{-2} \quad \text{and} \quad b = 1.677 \times 10^{-3} \pm 4.10^{-5}. \tag{30}$$

Results obtained with $k$ a correlation coefficient of 0.997 and an average error of ±8 °C.

### 5.3 Gas temperature in the base

At a given point, knowing the gas temperature, the change in the gas temperature is calculated gradually using the differentials defined before (Appendix 2). Annealing of 03 coils is considered (Fig. 10). The following equation should then be solved:

$$F\left(\theta_0^b\right) = 0 \tag{31}$$

The difficulty of this numerical resolution consists in finding a convergent algorithm. Indeed, a variation on $\theta_0^b$ makes only one weak variation on $F(\theta_0^b)$. However, after various numerical tests on $\theta_0^b$, the precision should be lower than one degree. If one uses the Newton's method which diverges because the precision of the derivative is not high enough. The dichotomic method converges for a too long calculation time. Good results are obtained by using the secant method [19]. The temperature $\theta_0^{cl}$ is given by the iterative process until convergence towards a value lower than $\xi_{gas}$.

$$\theta_0^{b^{n+1}} = \theta_0^{b^n} - \left(\theta_0^{b^n} - \theta_0^{b^{n-1}}\right)\frac{F(\theta_0^{b^n})}{F\left(\theta_0^{b^n}\right) - F\left(\theta_0^{b^{n-1}}\right)} \tag{32}$$

### 5.4 Radiative flux modeling

Radiation is an essential thermal transfer mode for the modeling of annealing bases. In the absence of multi reflexion, the expression of the flux received by the surface (Fig. 11) is:

$$\varphi_{1\Rightarrow 2} = \sigma\varepsilon_1\varepsilon_2F_{1\to 2}\left(T_{S1}^4 - T_{S2}^4\right) \tag{33}$$

The coils have an emissivity ranging between 0.5 and 0.7 while that of the bell is between 0.8 and 0.95. The bell, in the heating phase, radiates on all the furnace loads because the temperature of the wall is much higher than that of the coils. The radiative flux received on the surface of the crown $j$ of the coil is the sum of all fluxes leaving the crowns $i$ of the bell and falling on this crown $j$, therefore:

$$\varphi_j = \sum_{i=0}^{Nc}\sigma\varepsilon_i\varepsilon_jF_{i,j}\left(T_i^4 - T_j^4\right) \tag{34}$$

This flux $\varphi_j$, added to convective flux, will be introduced in the boundary conditions of the heat equation.

## 6 Validity of the measured gas cane temperature

Many dimensional checks of the gas temperatures show that the gas cane does not indicate really the gas temperature, except at the end of the annealing where the curves gas cane and gas temperature in the base meet (thermal homogeneity at the end of the annealing process). The gas cane, vis-a-vis of the burner, will be subjected to an intense radiation which will result in a rise of its rise temperature. Meanwhile, the gas will lose part of its calories by

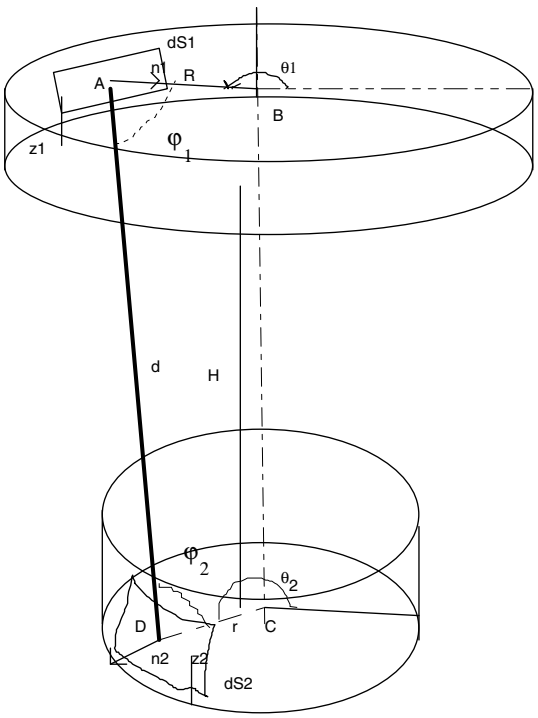


**Fig. 11** Schematization of the bell and a coil for radiative heat transfer calculation

convection. Due to the small size of the gas cane, one admits that it will reach, in a very short time, its equilibrium temperature (steady state). So, it could be stated that the heat received by radiation is equal to the heat yielded by convection. The heat received by radiation on the gas cane is the sum of 2 terms:

- a flux issued from the bell:

$$\varphi_{b\to cg} = F_{b\to cg}\varepsilon_{cg}\sigma\left(T_b^4 - T_{cg}^4\right) \tag{35}$$

- a flux resulting from the coil:

$$\varphi_{c\to cg} = F_{c\to cg}\varepsilon_{cg}\sigma\left(T_c^4 - T_{cg}^4\right) \tag{36}$$

As the gas cane is of small dimension, compared with the bell radius and with that of the coil radius, using approximation of the geometrical configuration, one obtains:

$$F_{b\to cg} = F_{c\to cg} = \frac{1}{2} \tag{37}$$

That is to say:

$$\varphi_{rad} = \frac{1}{2}\varepsilon_{cg}\sigma\left(T_b^4 + T_c^4 - 2T_{cg}^4\right) \tag{38}$$

The gas cane will yield a heat flux to the gas by convection according to Newton's law:

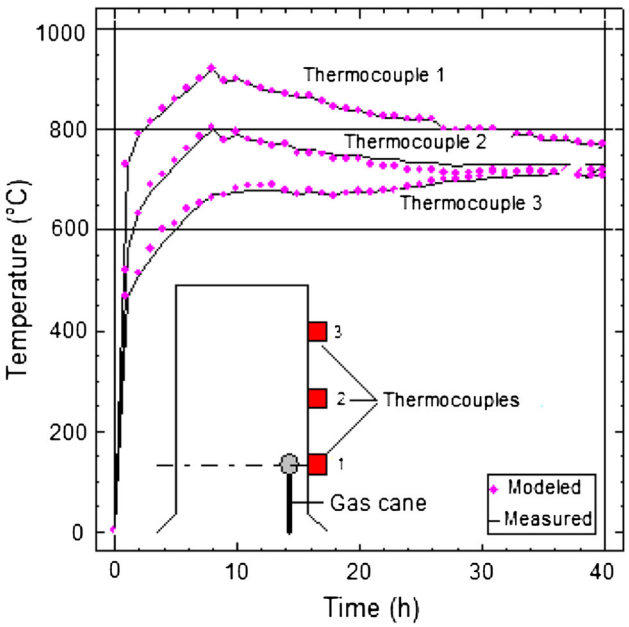


**Fig. 12** Measured and calculated values of temperature in the inner cover

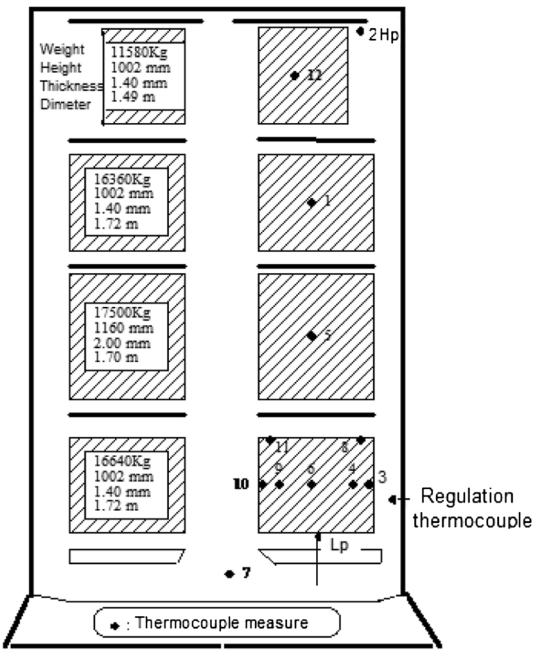


**Fig. 13** Embedded thermocouples location

$$\varphi_{conv} = h_{cg}\left(\theta_{cg} - \theta_g\right) \tag{39}$$

The convection coefficient for this geometry is obtained by Stasuilevichius formula [20]:

$$\Omega = 1 + 0.37\left[\frac{x_{cg}}{r_{cg}}\right]^{0.8} Re_r^{-0.2} \tag{40}$$

where

**Table 2** Experimental temperatures of the gas (E) and modeled temperatures (M) on the annealing base

| t (h) | Top coil convector (Hp 2 E) | Top coil convector (Hp 2 M) | Bell-face burner (B–B 3 E) | Bell-face burner (B–B 3 M) | Contact lower coil convector (Lp E) | Contact lower coil convector (Lp M) | Gas entrance (7 E) | Gas entrance (7 M) | Regulation thermo-couple (Reg) |
|---|---|---|---|---|---|---|---|---|---|
| 1 | 320 | 254 | 174 | 119 | 243 | 231 | 155 | 99 | 288 |
| 2 | 364 | 329 | 255 | 251 | 295 | 302 | 204 | 149 | 353 |
| 3 | 402 | 384 | 313 | 337 | 335 | 355 | 247 | 194 | 404 |
| 4 | 448 | 430 | 380 | 403 | 383 | 400 | 288 | 237 | 449 |
| 5 | 486 | 474 | 434 | 461 | 422 | 443 | 330 | 280 | 494 |
| 6 | 520 | 510 | 483 | 509 | 457 | 479 | 365 | 320 | 530 |
| 7 | 552 | 546 | 530 | 552 | 491 | 515 | 400 | 360 | 566 |
| 8 | 584 | 585 | 574 | 597 | 525 | 553 | 440 | 397 | 607 |
| 9 | 615 | 617 | 616 | 637 | 556 | 586 | 474 | 433 | 640 |
| 10 | 642 | 648 | 661 | 672 | 585 | 617 | 506 | 467 | 672 |
| 11 | 669 | 676 | 713 | 703 | 613 | 645 | 537 | 500 | 700 |
| 12 | 695 | 707 | 748 | 737 | 640 | 676 | 570 | 532 | 732 |
| 13 | 707 | 720 | 757 | 753 | 658 | 692 | 592 | 561 | 743 |
| 14 | 711 | 725 | 762 | 754 | 668 | 700 | 612 | 587 | 743 |
| 15 | 716 | 728 | 762 | 753 | 678 | 707 | 629 | 609 | 743 |
| 16 | 719 | 729 | 762 | 750 | 687 | 711 | 642 | 629 | 741 |
| 17 | 724 | 733 | 761 | 749 | 694 | 716 | 653 | 645 | 742 |
| 18 | 726 | 733 | 760 | 746 | 699 | 719 | 662 | 660 | 740 |
| 19 | 730 | 734 | 760 | 745 | 704 | 723 | 671 | 672 | 740 |
| 20 | 733 | 736 | 760 | 744 | 710 | 725 | 679 | 682 | 740 |
| 21 | 735 | 736 | 760 | 743 | 714 | 728 | 686 | 691 | 740 |
| 22 | 736 | 737 | 759 | 742 | 717 | 730 | 692 | 698 | 740 |
| 23 | 738 | 738 | 760 | 742 | 720 | 732 | 696 | 704 | 740 |

$$Re_r = \frac{\rho u r_{cg}}{\mu} \tag{41}$$

Then:

$$Nu_x = \frac{h_{cg} x_{cg}}{\lambda} = 0.0253 Re_x^{0.8} \Omega^{0.14} \left[\frac{\theta_g}{\theta_{cg}}\right]^{-0.25} \tag{42}$$

The heat balance between the radiative and the convective exchanges leads to the final formula allowing obtaining the gas temperature (Fig. 12):

$$\theta_g = \theta_{cg} - \frac{1}{2h_{cg}} \varepsilon_{cg} \sigma \left(T_b^4 + T_c^4 - 2T_{cg}^4\right) \tag{43}$$

## 6.1 Temperature distribution

The values of the measured gas temperature (E) and modeled (M) at different selected points of the base (Fig. 13): the top coil convector (Hp: point 2), the surface of the bell facing the burner (B–B: point 3), the lower coil convector (Lp), the gas entrance (Ge: point 7) and regulation thermocouple (Reg) are reported in Table 2. The temperature distribution of the gas versus time is plotted on the graph (Fig. 14).

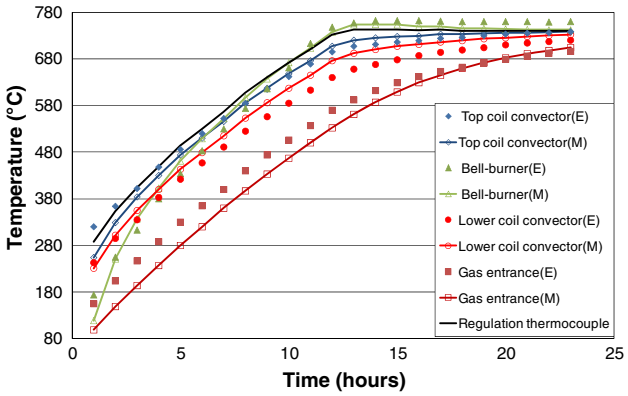


**Fig. 14** Experimental temperatures of the gas (E) and modeled temperatures (M) on the annealing base

## 7 Conclusion

Comparison between modeled flow rates and those measured confirmed the adequacy of the assumptions. There is a fairly marked similarity between modeling and testing of Kawasaki Steel. The presence of a slight shift in the curve has its origin in the geometry of the coil. The model pressure drops are close to the measurements thereby validating the coefficients of pressure drop.

The heat emitted by the furnace is described by a phenomenological model with two coefficients and a precision on the heating process of 8 °C. The model with the finite differences coupled to an iterative process made it possible to model the distribution of the temperature at any point in the gas of the annealing base.

## Appendix 1: Pressure drop coefficients

Using books and mementos [9–12], expressions of the pressure drop coefficients on all the singularities encountered in the annealing base are obtained.

- Gas entering in the pipe: $\chi = 0.5$
- Gas outlet in the pipe: $\chi = 1.06$
- Singular pressure drop upper coil: $\chi = 1$
- Pressure drop intrados: $\chi = 1$
- Singular pressure drop at the top of the bell: $\chi = 2$

Singular pressure drop stack top hat: the convector on top of stack, a hole was made to change the distribution of flows in base. Laboratory tests have estimated the pressure drops based on the ratio $\frac{d_{hp}}{D_{hp}}$ (Fig. 15). We modeled these losses by the regression formula

$$\chi = \frac{2.94506}{\left(d_{hp}/D_{hp}\right)^2} - \frac{0.47641}{\left(d_{hp}/D_{hp}\right)} \quad [9]$$

We introduce this formula into the calculation of pressure drops because the diameter of the orifice top of the stack $d_{hp}$, although the fixed construction; could be variable in order to better distribute the flow in the database.

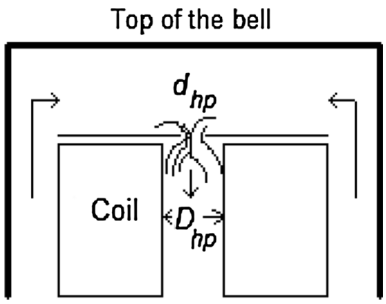


**Fig. 15** Schema of the top coil convector under the bell

Currently $\frac{d_{hp}}{D_{hp}} = \frac{100}{605} = 0.165$, gives a pressure drop coefficient $\chi = 105$.

## Appendix 2: Gas temperature calculation

The case of an annealing of 3 coils is taken into account (Fig. 10). The calculation of the temperatures will be carried out according to the 4 steps:

*Step 1* Knowing the temperature in $A$ $(\theta_g)$, one will calculate by Eq. (14) the temperature in the branch $\overline{AB}$. The temperature in $B$, $\theta_B$ is known.

*Step 2* Knowing the temperature in $A$ $(\theta_g)$, one will calculate by Eq. (14) the temperature in the branch $\overline{AC}$, and then $\theta_C$ is known.

*Step 3* Knowing the temperature at C, one will calculate by Eq. (17) the temperature in the branch $\overline{CK}$, and then the temperature $\theta_K$ in the branch is known. This same reasoning is continued to calculate sequentially $\theta_D, \theta_H, \theta_E, \theta_F$ by Eq. (19) and $\theta_G, \theta_N$ by Eq. (23).

*Step 4* Knowing $\theta_C$ and $\theta_H$, by Eq. (25), one will calculate $\theta_I$. By a similar reasoning one will calculate $\theta_I, \theta_L$ and $\theta_0$. If the ventilator block is at a thermal balance (low mass), then the temperature in $O$ is identical to the temperature in $P$ (the gas circulates in closed loop and the ventilator does not modify its temperature). The temperature in $B$ is not combined with the temperature of gas flow in $P$. The 4 steps make it possible to calculate the temperature in $P$ (exit ventilator diffuser) then, by propagation of heat along the gas circuit, the temperature in $O$ (entry ventilator diffuser). While supposing known: convection coefficients; temperatures of the walls (roughly, temperatures of the coils at the step $(t - \Delta t)$ resulting from the model of propagation of heat in a coil); velocities of the fluid (determined by the model of circulation of gas fluid at the step $(t - \Delta t)$; the bell temperature (known as a result of the temperature of the gas cane gas and at the temperature of the bell next the gas cane). Thus the temperature in $B$ (exit ventilator diffuser) is identical to the temperature in $P$ (entry ventilator diffuser). If $\theta_B \neq \theta_P$, then at least one of the parameters which models the thermal transfer is incorrect or unknown. By supposing the correct parameters, the only unknown parameter, but fixed in the algorithm at an arbitrary value, is $\theta_0^b$.

Three cases arise:

*Case 1* $\theta_P > \theta_B$, the gas was heated too much by licking the bell and thus the temperature of bell is too high. At the moment $t$ of the calculation, the temperature of the gas

cane is constant: according to Eq. (30), it is necessary to decrease $\theta_0^x$, and therefore $\theta_0^b$ too.

*Case 2* $\theta_B > \theta_P$, the gas was not heated enough by licking the bell. Thus the temperature of bell is not high enough. It is necessary to increase $\theta_0^b$.

*Case 3* $\theta_B = \theta_P$, the gas was heated sufficiently on the wall of the bell to guarantee the continuity of the temperatures along the gas circuit: $\theta_0^b$ is thus well adapted. It is a question of finding in such way that the difference between $\theta_B$ and $\theta_P$ is nil. Mathematically, the calculation algorithm of the temperature of gas can result in a real scalar function $F$ which at $\theta_0^b$ forward the value of $(\theta_B - \theta_P)$.

## References


1. Jaluria Y (1988) Numerical simulation of the transport processes in a heat treatment furnace. Int J Numer Methods Eng 25:387–399
2. Sabbonchi A, Hassanpour S (2008) Experimental and numerical investigation of coil heating in hydrogen annealing furnace for optimum arrangement of charge. Exp Heat Transf 21:220–235
3. Zou Y, Wu W, Zhang X, Lin L, Xiang S (2001) A study of heat transfer in high performance hydrogen bell-type annealing furnace. Heat Transf Asian Res 38(8):615–623
4. Tagliafico LA, Senarega M (2004) A simulation code for batch heat treatments. Int J Therm Sci 43:509–517
5. Sahay S, Kumar AM (2002) Applications of integrated batch annealing furnace simulator. Mater Manuf Process 17(4):439–453
6. Azimian AR, Kazimi AR (2005) Simulation of a box annealing unit. Int J Int Soc Scientometr Infometr 2(1):7–20
7. Sahay SS et al (2001) Development of an integrated batch annealing simulator for the CRM complex. Tata Search 64–71
8. Lopes AMG (2003) Implementation of the Hardy–Cross method for the solution of piping networks. Coimbra University, Coimbra, pp 117–125
9. Gilles RV, Evett JB, Liu C (1995) Mécanique des fluides et hydraulique. Mc Graw-Hill, Paris
10. Boussicaud A (1983) Calcul des pertes de charge. Chaud–Froid–Plomberie, Paris
11. Comolet R (1994) Mécanique expérimentale des fluides, Tome II: Dynamique des fluides réels; turbomachines. 4ème edn. Masson, Paris
12. Idel'cik IE (1986) Mémento des pertes de charge. Eyrolles, Paris
13. Grundmann D. The principles of fluid flow in a HPH bell-type annealing furnace. In: LOI high-performance hydrogen annealing colloquium, Technical University, Aachen
14. Kaihara T, Kawasaki T, Shiraishi N, Takeda S, Fujii S (1979) Optimum operation system of a batch type annealing furnace. Tetsu-to-Hagane 66(10)
15. Mo CL, Li Q, Guo XM, Wang H (2012) Numerical simulation the temperature field of the multi-coil batch during annealing process in bell-type furnace. Adv Mater Res 538–541:637–641
16. Chen G, Mingyan G (2007) Simulation of steel coil heat transfer in a high performance hydrogen furnace. Heat Transf Eng 28(1):25–30
17. Mc Adams WH (1967) Heat transmission. Mc Graw-Hill, New York
18. Krasnochtchekov E, Soukomel A (1985) Problèmes de transfert de chaleur. Mir, Moscou
19. Nougier JP (2001) Méthode de calcul numérique. Hermès Lavoisier, Paris
20. Gosse J (1981) Guide technique de thermique. Dunod, Paris